Journal of the American College of Cardiology
© 1999 by the American College of Cardiology
Published by Elsevier Science Inc.

Vol. 33, No. 3, 1999
ISSN 0735-1097/99/$20.00
PII S0735-1097(98)00602-0

EXPERIMENTAL STUDIES

Echocardiography-Derived Left Ventricular End-Systolic Regional Wall Stress and Matrix Remodeling After Experimental Myocardial Infarction

Luis E. Rohde, MD, MSc, Masanori Aikawa, MD, PhD, George C. Cheng, MD, PhD, Galina Sukhova, PhD, Scott D. Solomon, MD, FACC, Peter Libby, MD, FACC, Janice Pfeffer, PhD, Marc A. Pfeffer, MD, PhD, FACC, Richard T. Lee, MD, FACC

Boston, Massachusetts

OBJECTIVES We tested the hypothesis that regional end-systolic left ventricular (ESLV) wall stress is associated with extracellular matrix remodeling activity after myocardial infarction (MI).

BACKGROUND Increased left ventricular (LV) wall stress is a stimulus for LV enlargement, and echocardiography can be used to estimate regional wall stress. A powerful validation of a noninvasive method of estimating wall stress would be predicting cellular responses after a MI.

METHODS Echocardiographic images were obtained in rats 1, 7, 14 or 21 days after coronary ligation ($n = 11$) or sham surgery ($n = 5$). End-systolic left ventricular wall stress was calculated by finite element analysis in three regions (infarcted, noninfarcted and border) from short-axis images. Matrix metalloproteinase-9 (MMP-9) and macrophage density were determined by immunohistochemistry, and positive cells were counted in high power fields (hpf).

RESULTS Average ESLV wall stress was higher in rats with MI when compared to shams irrespective of time point ($p < 0.01$), and ESLV wall stress in the infarcted regions increased with time (25.1 ± 5.9 vs. 69.9 ± 4.4 kdyn/cm^2, day 1 vs. 21; $p < 0.01$). Matrix metalloproteinase-9 expression was higher in infarcted and border regions when compared to noninfarcted regions (22.1 vs. 25.7 vs. 0.10 cells/hpf, respectively; $p < 0.01$). Over all regions, ESLV wall stress was associated with MMP-9 ($r = 0.76$; $p < 0.001$), macrophage density ($r = 0.72$; $p < 0.001$) and collagen content ($r = 0.67$; $p < 0.001$). End-systolic left ventricular wall stress was significantly higher when MMP-9 positive cell density was greater than 10 cells/hpf (45 ± 20 vs. 14 ± 10 kdyn/cm^2; $p < 0.001$).

CONCLUSIONS Regional increases in ESLV wall stress determined by echocardiography-based structural analysis are associated with extracellular matrix degradation activity. (J Am Coll Cardiol 1999;33:835–42) © 1999 by the American College of Cardiology

Experimental and human studies have identified left ventricular (LV) remodeling as an important prognostic factor after myocardial infarction (MI) (1–4). The extent of ventricular dilation is directly related to the magnitude of the initial damage (5–7), but subsequent changes in ventricular geometry may also be dependent on the effect of distending forces and the tissue healing process (8). It has been postulated that LV wall stress may have important consequences in infarct expansion and further structural changes in LV geometry (5), although the cellular mechanisms of these effects are not fully understood.

To date, most noninvasive attempts to measure LV wall stress have been limited to two- and three-dimensional models that were represented by simplified geometry analyses (9,10). The accuracy of these simplified models is compromised in the setting of the complex geometrical deformations that occur in the infarcted ventricle (11). Finite element analysis, an engineering technique utilized to study complex structures, can overcome some of these limitations (12–15) and can be applied to echocardiographic images. Although computational biomechanical modeling such as finite element analysis probably adds accuracy to LV wall stress measurements, any modeling methodology should be supported by biological evidence.

Dynamic pathologic processes involving extracellular matrix rearrangement mediate many of the morphological

From the Cardiovascular Division, Department of Medicine, Brigham and Women's Hospital, Harvard Medical School, Boston, Massachusetts. Supported in part by grants from the National Heart, Lung, and Blood Institute (HL-54759 to R.T.L. and HL-48743 to P.L.) and the American Heart Association, National Center. Dr. Rohde was supported by Capes/Brasilia-Brazil. Dr. Solomon was supported by a Clinician Scientist Award from the American Heart Association.

Manuscript received January 30, 1998; revised manuscript received September 16, 1998, accepted November 5, 1998.

JACC Vol. 33, No. 3, 1999
March 1, 1999:835–42

Abbreviations and Acronyms

ESLV = end-systolic left ventricular
hpf = high power fields
LV = left ventricular
MI = myocardial infarction
MMP = matrix metalloproteinase
TIMP = tissue inhibitor of metalloproteinases

changes that occur after MI in both infarcted and peri-infarcted regions. Matrix metalloproteinases (MMPs) are a family of enzymes that play a crucial role in digestion of specific extracellular matrix components (16), and enhanced activity of MMPs have been demonstrated after experimental infarction (17).

In the absence of a reference standard for directly measuring stress, a powerful validation of a noninvasive method of estimating LV regional wall stress would be predicting regional pathophysiologic changes that follow an infarction. In addition, understanding the relationship between wall stress and MMP expression could provide insight into the role of mechanical forces in the processes involved in ventricular remodeling. The present study tested the hypothesis that focal MMP expression is associated with increased echocardiographically determined regional end-systolic left ventricular (ESLV) wall stress in an experimental model of MI.

METHODS

Animals and surgery. Thirty female Wistar rats, ranging in age from 8 to 12 weeks and in weight from 150 to 250 g, underwent coronary artery ligation for the production of MI. Overall survival rate was 53%. Only infarct sizes above 30% of the LV were used, resulting in 11 infarcted and 5 sham-operated animals that were included in the present study. Surgical procedures have been described in detail elsewhere (1). Briefly, animals were anesthetized with ether, intubated with a polyethylene endotracheal tube, and ventilated by a positive pressure rodent respirator (Columbus Inc., Columbus, Ohio). Following a left-sided thoracotomy, the heart was gently exteriorized and the left atrial appendage retracted to facilitate the ligation of the left coronary artery. In the sham procedure, a silk suture was inserted into the myocardium of the left ventricle and removed without ligation. All rats were housed under identical conditions and given food and water ad libitum.

Image acquisition and hemodynamic study. At each serial time point (1, 7, 14 and 21 days), groups of three to four rats were reanesthetized with ether to perform a hemodynamic study and to acquire echocardiographic images for structural analysis. The right carotid artery was cannulated with a 2-F Millar micromanometer that was advanced to the left ventricle. Echocardiographic and hemodynamic measurements were made under light ether anesthesia and spontaneous respiration. Short-axis two-dimensional echocardiographic images then were obtained with an ultrasound system (Sonos 1500; Hewlett-Packard Medical Products, Andover, Massachusetts) with a phased-array 5.0- to 7.5-MHz transducer. Three to five loops (each of them containing at least 10 heart beats) of LV short-axis images at the midpapillary level were recorded on S-VHS tapes. Simultaneously measurements of the systolic and end-diastolic LV pressures were made with image recordings.

Tissue collection. The rats were sacrificed immediately after the echocardiographic and hemodynamic studies. Their hearts were excised and the right and left ventricles were separated. A transverse section approximately 3 to 5 mm in length was obtained at the midventricular level, to assure the inclusion of papillary muscle sections. Tissue sections were embedded in O.C.T. compound (Miles, Elkhart, Indiana) and frozen in 2-methylbutane chilled with liquid nitrogen. Tissue blocks were stored at −80°C until sectioning.

Structural analysis. For each animal, the best transverse view of the left ventricle at the midpapillary level was chosen and, from the same frame at end-systole, the endocardial and epicardial contours were digitized. Digitized curves were imported into a computer simulations software package (IDEAS, SDRC, Inc.), and a solid surface and a finite element mesh were generated. The range of elements between models was 450 to 900, with a four-node brick element mesh. Loading conditions were applied to each individual element face on the endocardium. One node was restrained to move only in the radial direction, and one node next to the septum was restrained in all degrees of freedom. End-systolic left ventricular pressures measured simultaneously with image acquisition were used as loading pressures. The myocardial material properties were assumed to be homogeneous, isotropic and incompressible. A plane strain and minimal strain linear elastic finite element solution was employed. A Young's modulus of 2.1×10^8 kdyn/cm^2 was assumed to ensure a minimal strain model, and a Poisson's ratio of 0.49 represented near incompressibility. Von Mises stress, which represents a nondirectional parameter combining the effects of shear and normal forces, was calculated for each element and for the whole transverse section. In addition, changes in material properties were assigned to the infarcted segments according to previously reported estimates (18). Briefly, the models were solved with five- or 20-fold increases in the elastic modulus in the infarcted segment. The infarcted segment was spatially defined according to abrupt changes in wall thickness and wall motion analysis from the echocardiographic images. For simplicity, stresses derived from models that used a 20-fold increase in the elasticity modulus are reported here, as fivefold increases did not substantially change the solution from homogeneous models. Although the myocardium can behave as a nonlinear material, particularly during diastole, we did not incorporate nonlinearity,

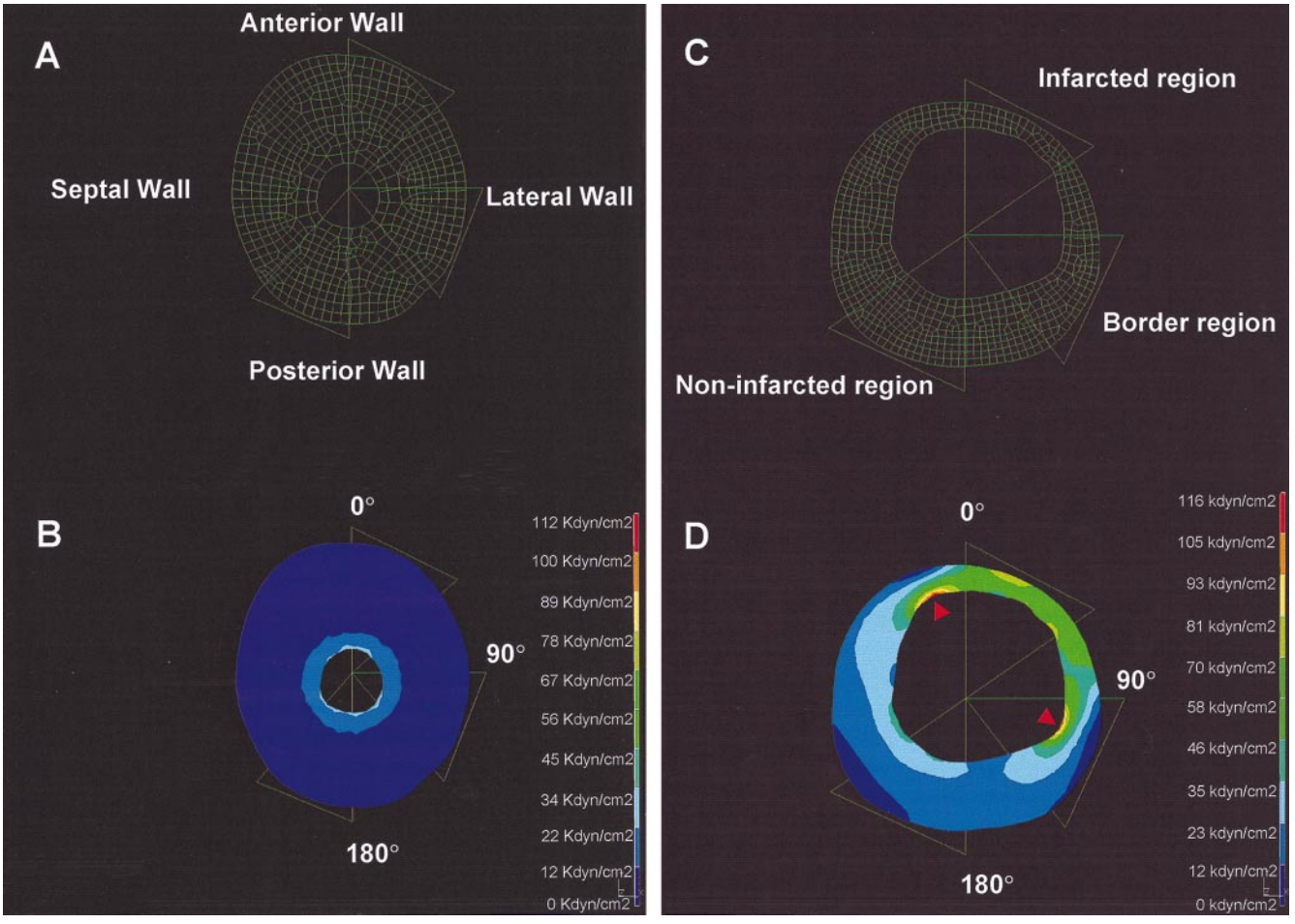

Figure 1. Representative examples of finite element meshes and color stress maps demonstrating the global and regional differences in left ventricular end-systolic wall stress between a sham-operated rat **(A** and **B)** and an infarcted rat **(C** and **D)** 21 days after the procedures. Each **triangle** designates the subdivisions of infarcted, border and noninfarcted regions, respectively. The same color scale was applied for both models. The left ventricle from the infarcted rat is dilated with focal areas of high ESLV stress concentrated in the regions that connect normal with infarcted tissue **(arrowheads)**.

because the left ventricle deformations were considered to be very small.

The main spatial marker used to guide the correlation between echocardiographic images and histologic sections was the location of the papillary muscles. The correlations were calculated based on the assumptions that 1) the dyskinetic areas by echocardiography correspond to areas with reduced thickness in histologic sections, and 2) the pattern of infarction in rats is generally predictable. Based on these assumptions, the models were evaluated in three different standard regions: infarcted, noninfarcted and border regions (Figure 1A and C). Regional Von Mises ESLV wall stress then was calculated in these subdivisions. To standardize this assessment, these three regions were measured beginning at 0°, 90° and 180°, respectively, in all models (Fig. 1C). Regional wall stress analysis was done in duplicate by the same observer; reproducibility exceeded 99%. In addition, wall thickness was also evaluated in the predefined regions, and a mean of three measurements in each segment was used for statistical analysis.

Immunohistochemistry. Staining was performed on frozen sections after fixation in cold acetone (−20°C). The sections were incubated with protein block serum-free (X0909; Dako Corp., California) for 5 min and then incubated with primary antibodies at room temperature for 1 h. After washing in phosphate-buffered saline, species-appropriate biotynilated secondary antibodies (E0464; Dako A/S, Denmark) were applied, followed by avidin–peroxidase complexes (Vector Laboratories). The following primary antibodies were used: monoclonal antihuman MMP-9 (2C10; British Biotech Co., United Kingdom), monoclonal antihuman tissue inhibitor of metalloproteinases-1 (TIMP-1) (IM32L; Oncogene Science) and monoclonal antirat macrophage (ED1, Serotec Ltd., United Kingdom).

From each section, cells positive for MMP-9 and macrophages were counted in three distinct high power field (hpf) pictures in each of the three predefined regions (infarcted, noninfarcted and border) in the infarcted rats and in three random regions in the sham-operated rats. Cell counts expressed as a mean of these three high power fields

JACC Vol. 33, No. 3, 1999
March 1, 1999:835–42

were used to calculate the associations. Cell counting was done blindly, and intraobserver reproducibility was greater than 95%.

Collagen content. Myocardium collagen area fraction was determined by quantitative morphometry of sirius red-stained sections. Fresh-frozen sections (6 μm) were rinsed with distilled water and incubated with 0.1% sirius red F3BA (Polyscience Inc., Warrington, Pennsylvania) in saturated picric acid. Sections were then rinsed with 0.01 N HCl for 1 min twice and then immersed in distilled water. After dehydration with 70% ethanol for 30 s, sections were visualized under polarized light and photographed with the same exposure time for each section. The predefined regions were scanned and analyzed by morphometry using a personal computer–based quantitative 24-bit (16.2 million unique combinations) color image analysis system. Collagen area fraction was calculated as the sum of all connective tissue divided by the sum of muscle areas and connective tissue in the visual field of the section. This approach predicts the proportion of myocardium occupied by fibrillar collagen and closely correlates with the hydroxyproline concentration of the tissue (19).

Statistical analysis. Data are presented as mean ± standard deviation. The two-tailed Student *t* test and analysis of variance were used to compare normally distributed continuous variables between groups. The Tukey test was used to correct for multiple comparisons. The association between regional LV wall stress and positive cell counts was evaluated by Spearman rank coefficients. $P < 0.05$ was considered statistically significant.

RESULTS

End-systolic left ventricular wall stress. Infarcted rats had significantly higher average ESLV wall stress when compared to sham-operated rats (29.0 ± 1.2 vs. 4.9 ± 11.6 kdyn/cm^2; $p = 0.001$, Fig. 1B and D), despite a consistent decrease in ESLV pressure (103 ± 11 vs. 112 ± 8 mm Hg in the shams; $p < 0.05$). Irrespective of the time point (n = 33 regions), infarcted regions showed a higher ESLV wall stress than border regions (42.2 ± 20 vs. 28.2 ± 12.5 kdyn/cm^2; $p < 0.01$), and border regions had higher levels than noninfarcted segments (28.2 ± 12.5 vs. 16.5 ± 6.5 kdyn/cm^2; $p < 0.01$). In general, LV wall stresses in both infarcted and border regions tended to increase with time. From day 1 to day 21, mean ESLV wall stress increased ($p < 0.01$) from 25.1 ± 5.9 to 69.9 ± 4.4 kdyn/cm^2 in the infarcted region, and tended to increase from 18.7 ± 5.5 to 37.9 ± 8.9 kdyn/cm^2 in the border region (Fig. 2).

Immunohistochemistry. Immunoreactive MMP-9 was detected in all infarcted rats in a reproducible pattern throughout the infarcted segments and border regions. Matrix metalloproteinase-9 expression was negligible in the sham-operated rats and in the noninfarcted regions of the infarcted rats (0.1 cell/hpf) and was higher in infarcted and

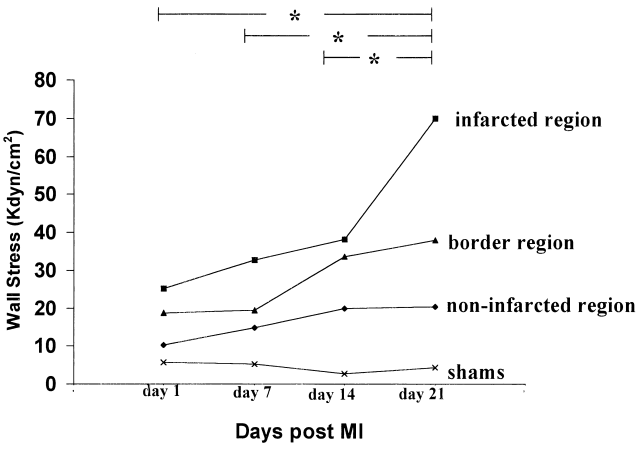

Figure 2. Temporal evolution of regional ESLV wall stress from day 1 to day 21 after the infarctions. Values for sham-operated rats are expressed as average of the entire transverse section. *$p < 0.05$ refers to comparisons within the infarcted segments between different time points. Regional wall stress increases progressively up to 3 weeks after the MI in the infarcted regions.

border regions when compared with noninfarcted regions (22.1 vs. 25.7 vs. 0.10 cells/hpf, respectively; $p < 0.01$). Expression on the 1st day after the infarction was modest and restricted to the border regions, but increased sharply after 7 days. From the 1st to the 7th day after the infarction, MMP-9 expression increased ($p < 0.05$) from 0.4 ± 0.5 to 49.3 ± 18.4 cells/hpf in the infarcted region and from 4.4 ± 1.3 to 37.8 ± 11.5 cells/hpf in the border region. Positive cells were still present 21 days after the infarction in both infarcted (33.8 ± 7.4/hpf; Fig. 3A) and noninfarcted regions (28.8 ± 1.5/hpf). Tissue inhibitor of metalloproteinases-1 immunoreactivity was found in smooth muscle cells surrounding intramyocardial vessels and in the same areas where collagen tended to accumulate (see below) in the infarcted rats 7, 14 and 21 days after the MI (Fig. 4).

Immunoreactive macrophage distribution resembled MMP-9 distribution. Positive cells were present mainly in the border regions on the 1st day after the MI, and peaked on the 7th day after the infarction (20.3 ± 18 vs. 71.2 ± 25.2 cells/hpf from day 1 to day 7; $p < 0.05$). Irrespective of the time point, positive cells were concentrated in the infarcted (39.7 ± 31.3 cells/hpf) and border regions (37.8 ± 22 cells/hpf; Fig. 3B); no positive cells were observed in the noninfarcted regions. Double immunostaining revealed that some macrophages expressed MMP-9 (Fig. 3C), although there were positive cells for MMP-9 that did not stain as macrophages and some macrophages that did not express MMP-9.

Collagen content. At the 1st day after the MI, there was a significant increase in collagen positive area in the infarcted segments when compared with sham-operated rats (4.8 ± 1.3 vs. 11.2 ± 2.9; $p < 0.01$) and, as expected, collagen content in the infarcted regions increased with time (11.2 ±

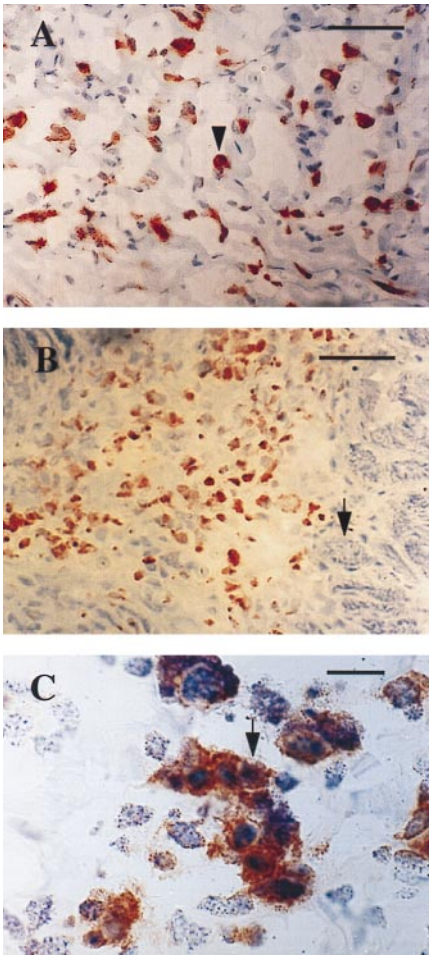

Figure 3. Immunohistochemistry for MMP-9 **(A)** and macrophages **(B)** in high power fields (×40, reduced by 65%). Matrix metalloproteinase-9 positive cells **(arrowheads)** are spread homogeneously throughout the infarcted region, and macrophages are shown infiltrating the border region next to myocardial cells **(arrow)**. Scale bars in **(A)** and **(B)** represent 55 μm. Double immunolabeling **(C)** for macrophages (blue-stained cells) and MMP-9 (red-stained cells) in high power fields (×100, reduced by 65%) demonstrates double-stained cells (purple cells, **arrow**). Scale bar in **(C)** represents 12 μm.

2.9 vs. 41.8 ± 15.5; from day 1 to day 21 $p < 0.05$). Collagen tended to accumulate next to the endocardial and epicardial surface and, interestingly, away from the regions where MMP-9 was expressed (Fig. 4).

Matrix metalloproteinase-9 and macrophages versus regional LV wall stress. As we identified an increased focal expression of immunoreactive MMP-9 and macrophages after the infarctions, we hypothesized that echocardiography-based left ventricular wall stress distribution would correlate with these two biological variables. The associations between MMP-9 and macrophage cell density with ESLV wall stress were analyzed among all predefined regions of infarcted and sham-operated rats at all time points after infarction. Regional LV wall stress among these regions correlated significantly with the number of cells stained for MMP-9 (Spearman coefficient = 0.76; $p < 0.001$). A significant correlation was also shown between macrophage expression and regional wall stress ($r = 0.72$; $p < 0.001$). These associations were also significant when the regions were dichotomized according to the density of positive cells. Regions with more than 10 positive cells/hpf for MMP-9 and macrophages had significantly higher regional ESLV wall stress than those with less than 10 cells/hpf (45.1 ± 20.1 vs. 14.3 ± 10.4 kdyn/cm^2 for MMP-9, $p < 0.001$; and 41.1 ± 19.7 vs. 12.6 ± 9.6 kdyn/cm^2 for macrophages, $p < 0.001$; Fig. 5). Regional collagen content was also positively associated with regional wall stress ($r = 0.67$; $p < 0.001$). Finally, wall thickness was weakly and inversely associated with regional ESLV wall stress ($r = -0.33$; $p = 0.02$), and ESLV pressure was not significantly associated with average stress ($r = 0.14$; $p = 0.6$).

Varying material properties. When the models were solved with a 20-fold increase in the elastic modulus of the infarcted tissue, there was a consistent increase in wall stress of the infarcted regions with minor changes in the noninfarcted segments. With this approach, the association between regional wall stress with MMP-9 expression ($r = 0.79$; $p < 0.001$), macrophage positivity ($r = 0.76$; $p < 0.001$) and collagen content ($r = 0.68$; $p < 0.001$) remained highly statistically significant.

DISCUSSION

In this study of experimental MI, we identified a progressive increase in regional ESLV wall stress associated with the expression of immunoreactive MMP-9 and macrophage infiltration. Compelling evidence implicates both extracellular matrix degradation and mechanical forces in the geometrical changes that occur in the infarcted ventricle (5,17). Noninvasive methods of studying LV regional wall stress may provide important information that global measures of LV function and wall stress lose. Our data suggest that regional ESLV wall stress can identify areas where biological processes are active with a higher predictive power than the simpler parameters systolic wall thickness and LV pressure.

Wall stress measurements. Myocardial stress has been traditionally viewed as an important stimulus for the remodeling of the heart, but even in the open chest animal, direct stress measurements are technically difficult (20). Noninvasive estimates of average stress in the left ventricle have proven useful in numerous clinical settings, such as evaluating contractile function in the presence of valvular disease (21–23). These estimates of LV wall stress are based on idealized LV geometries and are particularly useful when studying LV contractility under different loading conditions. However, these simplified analytic methods cannot estimate regional stress in distorted ventricles. The association of increased regional wall stress with MMP expression, macrophage density and collagen content described by

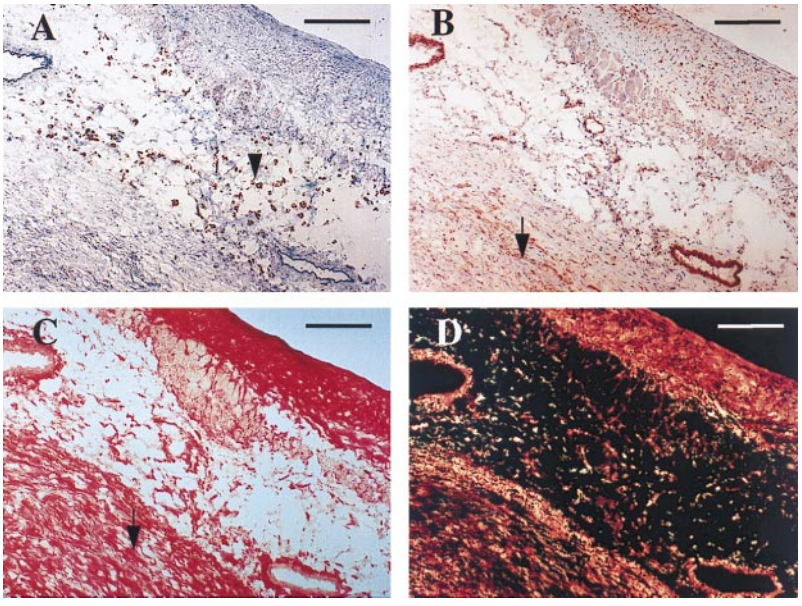

Figure 4. Sections of an infarcted segment 21 days after the surgery showing MMP-9 **(A)** and TIMP-1 **(B)** immunoreactivity. Parallel sections demonstrate collagen accumulation under direct **(C)** and under polarized light **(D)**. Note dissociation between the areas that express MMP-9 **(arrowheads)** and the areas that express TIMP-1 **(arrow)** and are rich in collagen **(arrow)**. Scale bars represent 70 μm.

the current study provides experimental evidence supporting the concept that focal increases in wall stress represent areas of remodeling activity.

In previous studies, finite element analysis of regional LV stress has correlated with stress calculations based on models of the left ventricle represented as a noncircular cylinder with nonuniform thickness and increasing geometrical complexity (24). Lessick et al. (25) used magnetic resonance imaging and finite element analysis to demonstrate that wall stress indices increased after acute experimental ischemia, predominantly in the ischemic segments. Our data support the concept that wall stress in the infarcted area increases substantially after an acute ischemic insult and that this increase is sustained and progressive up to three weeks after the MI. Recently, finite element analysis has also been used to study LV mechanics in three-dimensional reconstruction of the canine left ventricle. These studies demonstrated that prestretching of the myocardial laminae may be a primary mechanism of residual shear stress, and that there is significant nonhomogeneity of fiber stress through different regions of the ventricle (14,15).

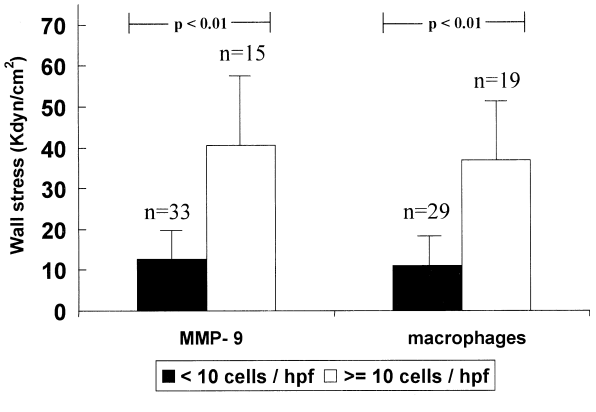

Figure 5. The relationship between ESLV wall stress with MMP-9 and macrophage content dichotomized according to the density of positive cells. "N" represents the number of segments analyzed. Regions with more than 10 cells/high power field (hpf) have a threefold increase in regional ESLV wall stress when compared to regions with fewer positive cells.

Extracellular matrix remodeling. The morphological rearrangement that occurs after a MI is partially mediated by pathologic processes involving reorganization of extracellular matrix components (26–28). Cleutjens et al. demonstrated a transient increase in collagenase activity in the infarcted left ventricle which began two days after the infarction, peaked at day seven and declined thereafter, together with a concomitant contribution in collagenolytic activity from gelatinases (MMP-9 and MMP-2) (17). Studies of collagen content after experimental MI also emphasize the importance of the balance between collagen synthesis and degradation in LV remodeling (28–30). In our study, MMP-9, TIMP-1 and collagen content were evaluated as mediators of the degradation pathways involved in this balance. Interestingly, regions where collagen was densely accumulated and organized were adjacent to but distinct from the areas where MMP-9 and macrophages were present. The source of MMP-9 and other MMPs in intact and damaged myocardial tissue is incompletely defined. It has been suggested that the cells responsible for MMP-13 transcription in a rat model of infarction are fibroblast-like cells and not leukocytes or endothelial cells

(17). However, many other cells, such as neutrophils, fibroblasts and other stromal cells, can produce MMPs (30,31) in the infarcted and peri-infarcted tissue. Matrix metalloproteinase synthesis is under intricate control, involving a variety of physiologic and pharmacologic stimuli, and some evidence suggests that mechanical events could contribute to this regulation. James et al. (32) demonstrated induction of collagenase gene expression by mechanical injury in vascular smooth muscle cells. In human atherosclerotic coronary lesions, overexpression of MMP-1 occurs in regions of increased circumferential stress in the fibrous cap (33).

Limitations. In this study, ESLV wall stress measurements were based on two-dimensional short-axis reconstructions of infarcted left ventricles. Although the association between stress and matrix remodeling activity was very good, three-dimensional reconstructions could theoretically add additional accuracy to the stress calculations. It is also important to note that we chose Von Mises stress as the stress parameter, as this scalar stress parameter does not depend on the coordinate system. The authors acknowledge that most biological materials are frequently nonlinear, and the diastolic myocardium in particular is highly nonlinear and has both viscoelastic and poroelastic passive properties. Nonlinearity was not incorporated in this study because the constitutive equations for peak or end-systolic myocardial behavior are incompletely described. In addition, the left ventricle was modeled at end-systole as quasi-steady, that is, it is expected that the stiffness component dominates any viscous or inertial contributions. The maximum strains would be so small that even a highly nonlinear material law would yield identical results. The models also assumed that the stress-free state is the same as the end-systolic state. The presence of residual stress could potentially have interfered with our results (14,34).

Conclusions. We have demonstrated that regional overexpression of MMP-9 and accumulation of macrophages and collagen correlate with increased mechanical stress (end-systolic) in the infarcted left ventricle. The associations observed in this study, however, do not establish a cause and effect relationship. Further studies are needed to understand the pathways by which mechanical forces can result in expression of MMPs and activate the remodeling process.

Acknowledgments

The authors gratefully acknowledge the expert technical assistance of Dr. Peter Finn, Dr. Elena Rabkin and Joseph Gannon.

Reprint requests and correspondence: Dr. Richard T. Lee, Cardiovascular Division, Brigham and Women's Hospital, 75 Francis St., Boston, Massachusetts 02115 USA. E-mail: rtlee@bics.bwh.harvard.edu.

REFERENCES

1. Pfeffer JM, Pfeffer MA, Fletcher PJ, Braunwald E. Progressive ventricular remodeling in rat with myocardial infarction. Am J Physiol 1991;260:H1406–14.
2. Pfeffer MA, Pfeffer JM, Steinberg C, Finn P. Survival after an experimental myocardial infarction. Beneficial effects of long term therapy with captopril. Circulation 1985;72:406–12.
3. White HD, Norris RM, Brown MA, Brandt PWT, Whitlock RML, Wild CJ. Left ventricular end systolic volume as the major determinant of survival after recovery from myocardial infarction. Circulation 1987;76:44–51.
4. Hammermeister KE, DeRouen TA, Dodge HT. Variables predictive of survival in patients with coronary disease. Selection by univariate and multivariate analyses from clinical electrocardiographic, exercise, arteriographic, and quantitative angiographic evaluations. Circulation 1979;59:421–30.
5. Pfeffer MA, Braunwald E. Ventricular remodeling after myocardial infarction. Experimental observations and clinical implications. Circulation 1990;81:1161–72.
6. Kostuk WJ, Kazamias TM, Gander MP, Simon AL, Ross J. Left ventricular size after myocardial infarction. Serial changes and their prognostic significance. Circulation 1973;47:1174–9.
7. Stone PH, Raabe DS, Jaffe AS, et al. Prognostic significance of location and type of myocardial infarction. Independent adverse outcome associated with anterior location. J Am Coll Cardiol 1988;11:453–63.
8. Rumberger JA. Ventricular dilatation and remodeling after myocardial infarction. Mayo Clin Proc 1994;69:664–74.
9. Wong AYK, Rautarharju PM. Stress distribution within the left ventricular wall approximated as a thick ellipsoidal shell. Am Heart J 1968;75:649–62.
10. Moriarty TF. The law of Laplace, its limitations as a relation for diastolic pressure, volume or wall stress of the left ventricle. Circ Res 1980;46:321–31.
11. Solomon SD, Martini M, Rosario L, et al. Regional wall stress following myocardial infarction estimated by echocardiography-based structural analysis. J Am Soc Echocardiog 1998;32:1819–24.
12. Janz RF, Grimm AF. Finite-element model for the mechanical behavior of the left ventricle. Circ Res 1972;30:244–52.
13. Bovendeerd PH, Arts T, Delhaas T, et al. Regional wall mechanics in the ischemic left ventricle: numerical modeling and dog experiments. Am J Physiol 1996;270:H398–10.
14. Costa KD, May-Newmn K, Farr D, et al. Three-dimensional residual strain in midanterior canine left ventricle. Am J Physiol 1997;273:H1968–76.
15. Guccione JM, Costa KD, McCulloch AD. Finite element stress analysis of left ventricular mechanics in the beating dog heart. J Biomech 1995;28:1167–77.
16. Tyagi SC, Ratajska A, Weber KT. Myocardial matrix metalloproteinases: localization and activation. Mol Cell Biochem 1993;126:49–59.
17. Cleutjens JPM, Kandala JC, Guarda E, Guntaka RV, Weber KT. Regulation of collagen degradation in the rat myocardium after infarction. J Mol Cell Cardiol 1995;27:1281–92.
18. Gupta KB, Ratcliffe MB, Fallert MA, Edmunds LH, Bogen DK. Changes in passive mechanical stiffness of myocardial tissue with aneurysm formation. Circulation 1994;89:2315–26.
19. Grilla CG, Pick R, Tan LP, Janicki JS, Weber KT. Remodeling of rat right and left ventricles in experimental hypertension. Circ Res 1986;58:38–46.
20. Janz RF. Estimation of local myocardial stress. Am J Physiol 1982;242:H875–81.
21. St. John Sutton MG, Plappert TA, Hirshfield JW, Reichek

N. Assessment of left ventricular mechanics in patients with asymptomatic aortic regurgitation: a two-dimensional echocardiographic study. Circulation 1984;69:259–68.
22. Zile MR, Gaasch WH, Carroll JD, Levine HJ. Chronic mitral regurgitation: predictive value of preoperative echocardiographic indexes of left ventricular function and wall stress. J Am Coll Cardiol 1984;3:235–42.
23. Reichek N, Wilson J, St. John Sutton M, Plappert TA, Goldberg S, Hirshfield JW. Noninvasive determination of left ventricular end-systolic stress: validation of the method and initial application. Circulation 1982;65:99–108.
24. Janz RF, Ozpetek S, Ginzton LE, Laks MM. Regional stress in a noncircular cylinder. Biophys J 1989;55:173–82.
25. Lessick J, Sideman S, Azhari H, Shapiro E, Weiss JL, Beyar R. Evaluation of regional load in acute ischemia by three dimensional curvatures analysis of the left ventricle. Ann Biomed Eng 1993;21:147–61.
26. Cannon RO III, Butany JW, McManus BM, et al. Early degradation of collagen after myocardial infarction in the rat. Am J Cardiol 1983;52:390–5.
27. Dixon IMC, Ju H, Jassal DS, Peterson DJ. Effect of ramipril and losartan on collagen expression in right and left heart after myocardial infarction. Mol Cell Biochem 1996;165:31–45.
28. Shieffer B, Wirger A, Meybrum M, et al. Comparative effects of chronic angiotensin-converting enzyme inhibition and angiotensin II type 1 receptor blockade on cardiac remodeling after myocardial infarction in the rat. Circulation 1994;89:2273–82.
29. Cleutjens JPM, Verluyten MJA, Smits JFM, Daemen MJAP. Collagen remodeling after myocardial infarction in the rat heart. Am J Pathol 1995;147:325–38.
30. Campbell EJ, Cury JD, Shapiro SD, Goldberg GI, Welgus HC. Neutral proteinases of human mononuclear phagocytes. Cellular differentiation markedly alters cell phenotype for serine proteinases, metalloproteinases, and tissue inhibitor of metalloproteinases. J Immunol 1991;146:1286–93.
31. Shapiro SD, Campbell EJ, Senior RM, Welgus HC. Proteinases secreted by human mononuclear phagocytes. J Rheumatol 1991;18:95–8.
32. James TW, Wagner R, White LA, Zwolak RM, Brinckerhoff CE. Induction of collagenase and stromelysin gene expression by mechanical injury in a vascular smooth muscle-derived cell line. J Cell Physiol 1993;157:426–37.
33. Lee RT, Schoen FJ, Loree HM, Lark MW, Libby P. Circumferential stress and matrix metalloproteinase 1 in human coronary atherosclerosis. Implications for plaque rupture. Arterioscler Thromb Vasc Biol 1996;16:1070–3.
34. Fung YC. The heart—the need for a new hypothesis for residual stress distribution. In: Fuang YC, editor. Biodynamics. Circulation. New York: Springer-Verlag, 1984:22–76.